Radio interferometry

Kaj Wiik

Tuorla Observatory

Summer 2018

Based partly on 'Essential radio astronomy' from http://www.cv.nrao.edu/course/astr534/Interferometers1.html and http://www.cv.nrao.edu/course/astr534/Interferometers2.html by J. J. Condon and S. M. Ransom.

Outline

Interferometry-2

Sensitivity and amplitude calibration

Imaging - modelfitting

Sensitivity I

Antenna response:

$$K = \frac{\eta_a A}{2k} 10^{-26} = \frac{A_{eff}}{2k} 10^{-26} = \frac{T_a}{S} \left[\frac{\mathrm{K}}{\mathrm{Jy}} \right] = \mathrm{DPFU} \qquad (1)$$

System response **SEFD**: what amount of source flux increases the system noise as much as the noise of the receiving equipment when $T_a = 0$:

$$\mathrm{SEFD} = \frac{T_{sys}}{\mathrm{DPFU}} = \frac{2kT_{sys}}{A_{eff}} \cdot 10^{-26} \quad [\mathrm{Jy}] \qquad (2)$$

Baseline sensitivity for antennas i and j (η_s = system efficiency):

$$\Delta S_{ij} = \frac{1}{\eta_s} \sqrt{\frac{\mathrm{SEFD}_i \cdot \mathrm{SEFD}_j}{2\Delta\nu\tau_{int}}} \quad [\mathrm{Jy}] \qquad (3)$$

Sensitivity II

The number of baselines L is:

$$L = \frac{1}{2} \cdot N \cdot (N-1), \tag{4}$$

where N = number of antennas.

Image sensitivity I_m is standard deviation of mean of L samples (baselines),

$$\Delta I_m = \frac{1}{\eta_s} \sqrt{\frac{\mathrm{SEFD}_i \cdot \mathrm{SEFD}_j}{N(N-1)\Delta\nu\tau_{int}}} \quad [\mathrm{Jy/beam}] \tag{5}$$

Imaging

There are three basic methods to produce images from interferometry data:

- Fitting a source model to the visibilities.
  - Possible to get images even from a noisy and sparse dataset.
  - Accurate source parameters: emission component sizes, shapes, and locations.
- Inverse transform of the visibilities and deconvolution.
  - No a-priori control of source shape $\Rightarrow$ somewhat more objective approach.
  - Clean (many variants), maximum entropy method (MEM) most important deconvolution methods.
- Direct inversion using **Compressed Sensing** algorithms (in development)

Sampling of the (u,v) plane

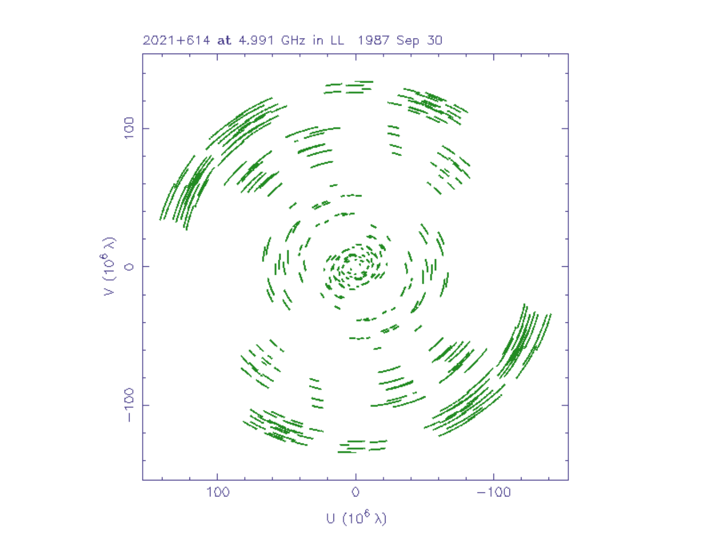

Visibility versus (u,v) radius

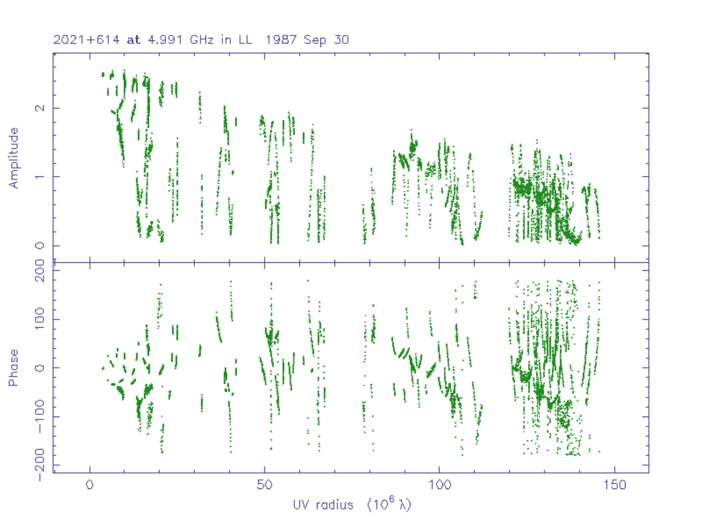

The University of New Mexico

Visibility versus time

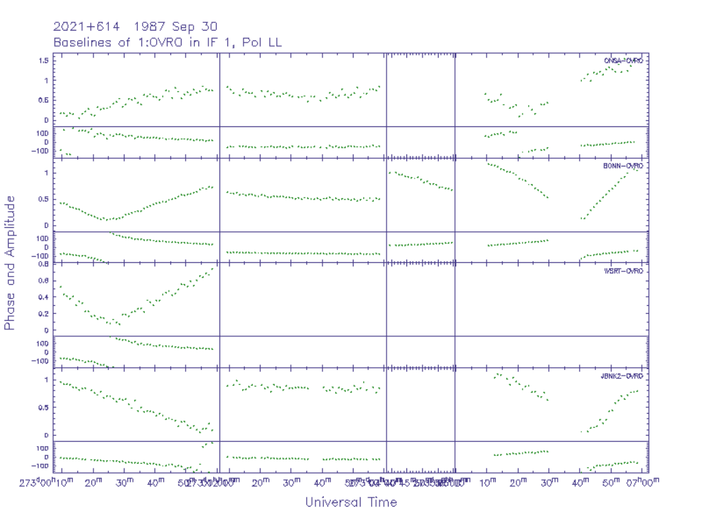

Amplitude across the (u,v) plane

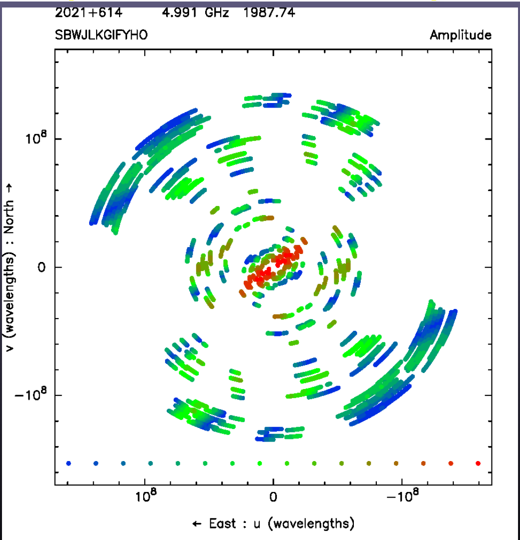

Projection in the (u,v) plane

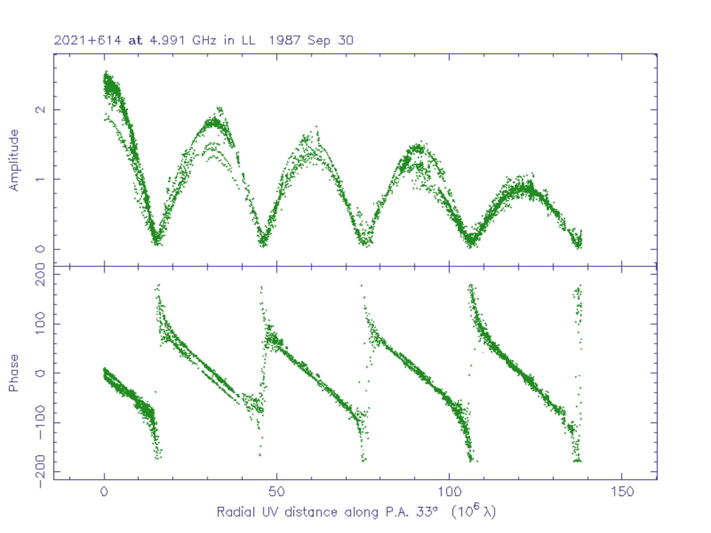

Fourier transform properties

$$F(u,v) = \mathrm{FT}\{f(x,y)\}$$

i.e.,

$$F(u,v) = \int_{-\infty}^{\infty}\int_{-\infty}^{\infty} f(x,y)\exp[2\pi i(ux+vy)]\,dx\,dy$$

Linearity

$$\mathrm{FT}\{f(x,y)+g(x,y)\} = F(u,v) + G(u,v)$$

Convolution

$$\mathrm{FT}\{f(x,y)\star g(x,y)\} = F(u,v)\cdot G(u,v)$$

Shift

$$\mathrm{FT}\{f(x-x_i, y-y_i)\} = F(u,v)\ \exp[2\pi i(ux_i+vy_i)]$$

Similarity

$$\mathrm{FT}\{f(ax,by)\} = \frac{1}{|ab|}F\left(\frac{u}{a},\frac{v}{b}\right)$$

Component profiles

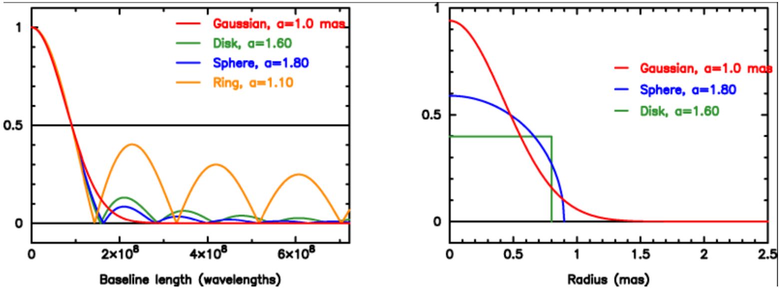

There is very little difference in the uv-plane between different source profiles down to the relative half flux level.

Simple source structures

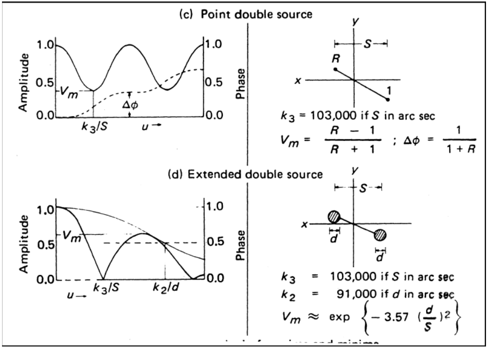

Component separation from the uv-radius (in wavelengths) of the first valley (k3/S), size of individual emission region (d [arcsec]) from the uv-radius of the half-value point of the envelope (k2/d). Amplitude is normalized.

Simple source structures, example

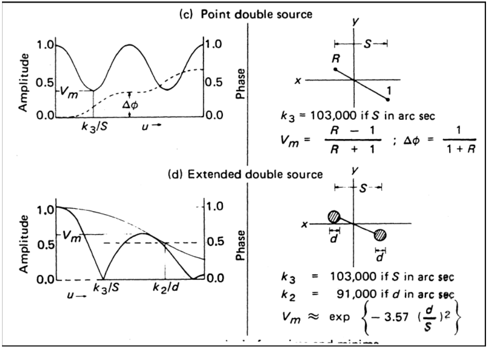

First valley at 100 M$\lambda = k_3/S$, envelope half-value point 300 M$\lambda = k_2/d$.

Double source, component separation
$S = k3/100\mathrm{M}\lambda = 103000/100e6 = 0.001\,\mathrm{arcsec} = 1\,\mathrm{marcsec}.$

Component size
$d = k2/300\mathrm{M}\lambda = 91000/300e6 = 0.0003\,\mathrm{arcsec} = 300\,\mu\mathrm{arcsec}$

Simple source structures in 2D

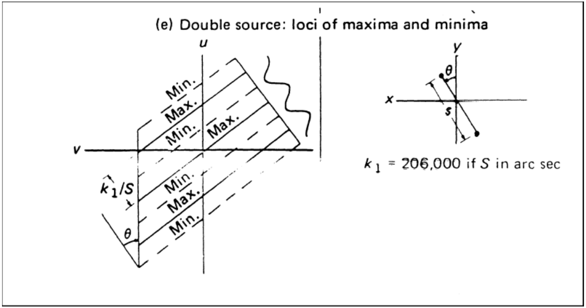

Component separation from the valley-to-valley distance (k1/S).

Source shift

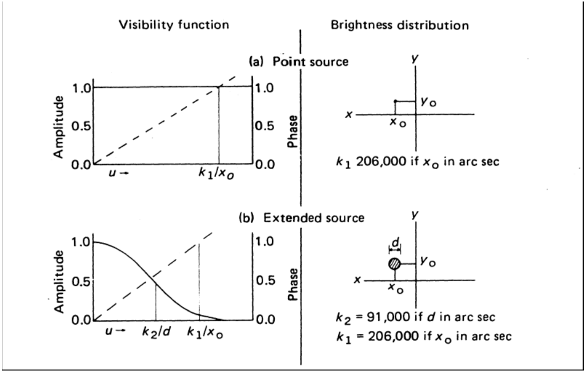

Trial model

- By inspection, we can derive a simple model:
- Two equal components, each 1.25 Jy, separated by about 6.8 milliarcsec in p.a. 33º, each about 0.8 milliarcsec in diameter (Gaussian FWHM)
- *To be refined later.*

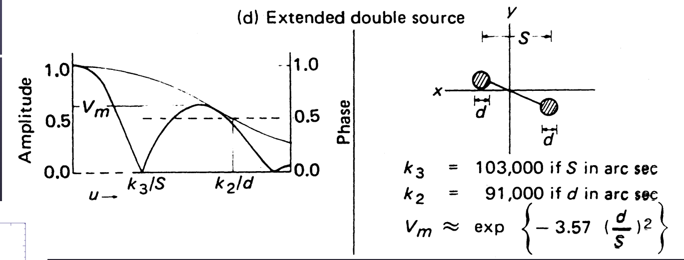

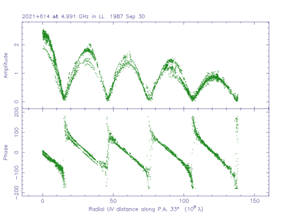

Projection in the (u,v) plane

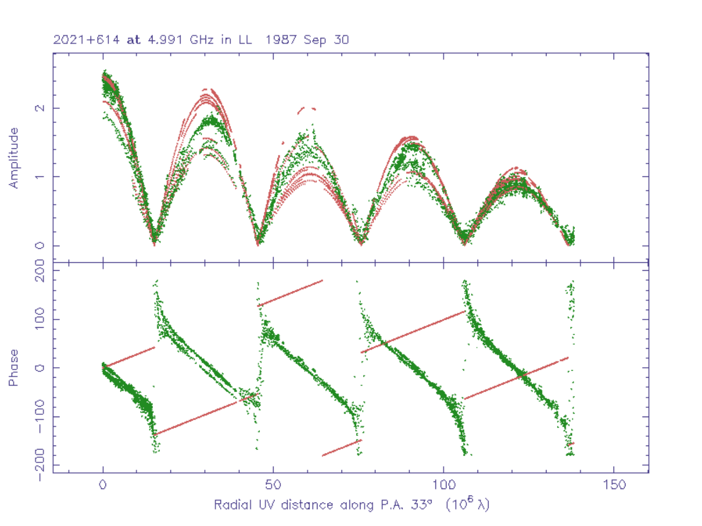

Parameters

- Example
  - Component position: (*x,y*) or polar coordinates
  - Flux density
  - Angular size (e.g., FWHM)
  - Axial ratio and orientation (position angle)
    - For a non-circular component
  - 6 parameters per component, plus a "shape"
  - This is a conventional choice: other choices of parameters may be better!
  - (Wavelets; shapelets* [Hermite functions])
    - * Chang & Refregier 2002, ApJ, 570, 447

Practical model fitting: 2021

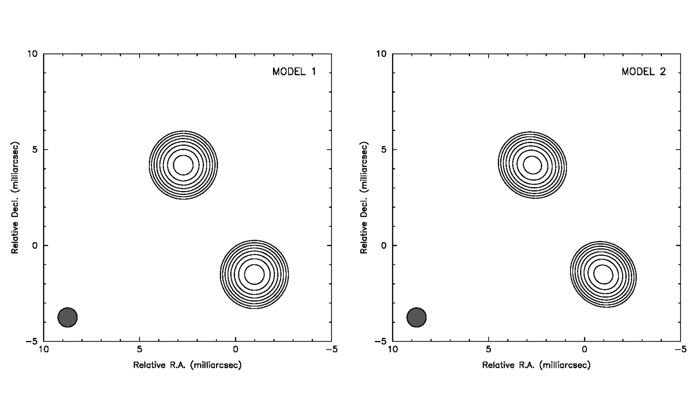

! Flux (Jy)	Radius (mas)	Theta (deg)	Major (mas)	Axial ratio	Phi (deg)	T
1.15566	4.99484	32.9118	0.867594	0.803463	54.4823	1
1.16520	1.79539	-147.037	0.825078	0.742822	45.2283	1

2021: model 2

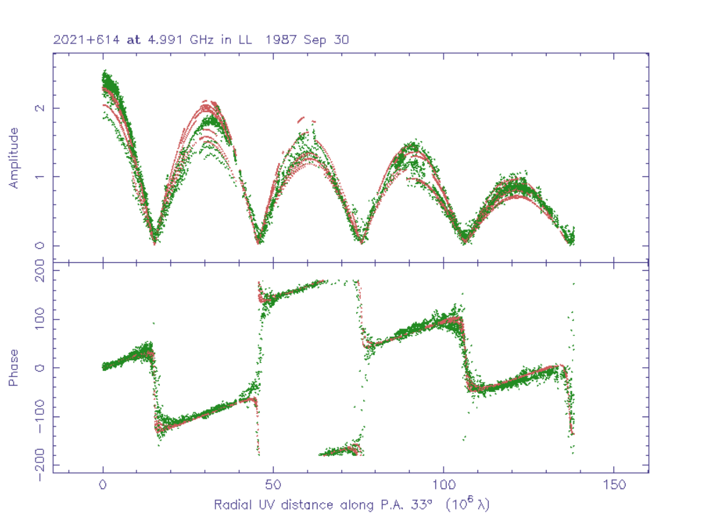
2021+614 at 4.991 GHz in LL 1987 Sep 30
Amplitude
Phase
Radial UV distance along P.A. 33° (10^6 λ)
0
1
2
200
100
0
−100
−200
0
50
100
150

Model fitting 2021

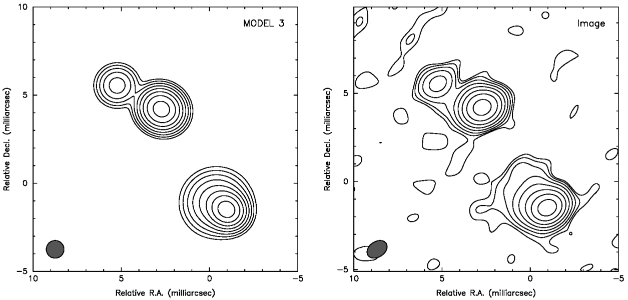

! Flux (Jy)	Radius (mas)	Theta (deg)	Major (mas)	Axial ratio	Phi (deg)	T
1.10808	5.01177	32.9772	0.871643	0.790796	60.4327	1
0.823118	1.80865	-146.615	0.589278	0.585766	53.1916	1
0.131209	7.62679	43.3576	0.741253	0.933106	-82.4635	1
0.419373	1.18399	-160.136	1.62101	0.951732	84.9951	1

2021: model 3

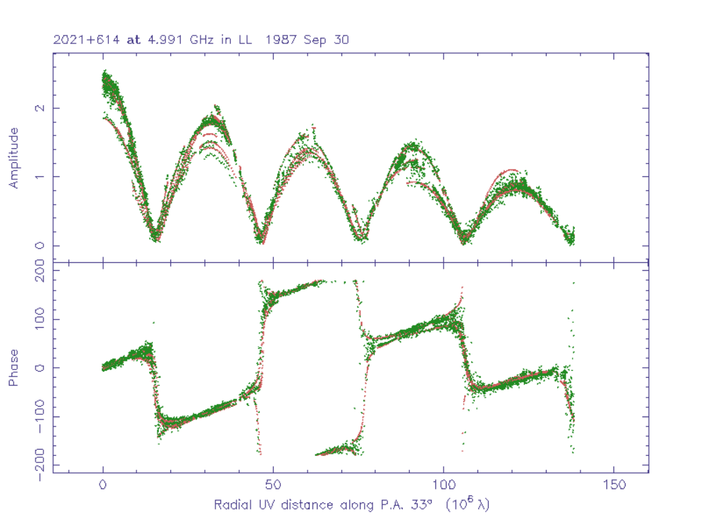
2021+614 at 4.991 GHz in LL 1987 Sep 30
Amplitude
Phase
Radial UV distance along P.A. 33° (10^6 λ)
0
1
2
200
100
0
−100
−200
0
50
100
150

Example: Space radio interferometry

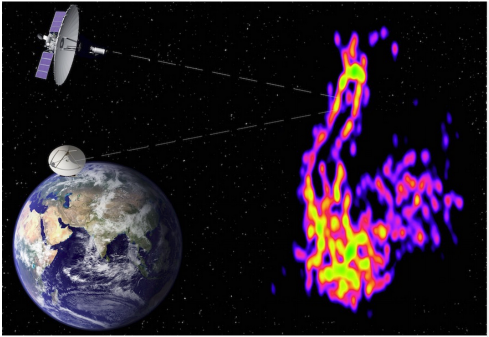

Yhdistämällä useita teleskooppeja toisiinsa pystyttiin ottamaan ennätystarkka kuva mustan aukon suihkusta. Kuva Pier Raffaele Platania INAF/IRA (kompositio); Lebedev Instituutti (RadioAstron)

03.04.2018 | Sakari Nummila

Tähtitieteilijät loivat maapalloa suuremman teleskoopin

Tuomas Savolainen käytti tähtitieteen historian tarkinta havaintolaitetta tutkiakseen mustan aukon synnyttämää plasmasuihkua. Tulokset paljastivat uutta tietoa jättiläismäisten suihkujen rakenteesta.

Example: Space radio interferometry

nature.com > nature astronomy > letters > article

MENU

nature astronomy

Letter

A wide and collimated radio jet in 3C84 on the scale of a few hundred gravitational radii

G. Giovannini, T. Savolainen, M. Orienti, M. Nakamura, H. Nagai, M. Kino, M. Giroletti, K. Hada, G. Bruni, Y. Y. Kovalev, J. M. Anderson, F. D'Ammando, J. Hodgson, M. Honma, T. P. Krichbaum, S.-S. Lee, R. Lico, M. M. Lisakov, A. P. Lobanov, L. Petrov, B. W. Sohn, K. V. Sokolovsky, P. A. Voitsik, J. A. Zensus & S. Tingay

Nature Astronomy **2**, 472–477 (2018)
doi:10.1038/s41550-018-0431-2
Download Citation

Received: 16 October 2017
Accepted: 27 February 2018
Published: 02 April 2018

Example: Space radio interferometry

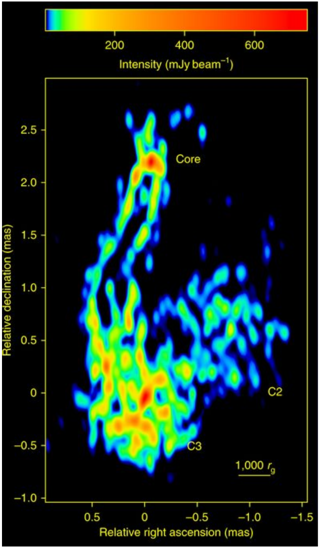

Example: Space radio interferometry

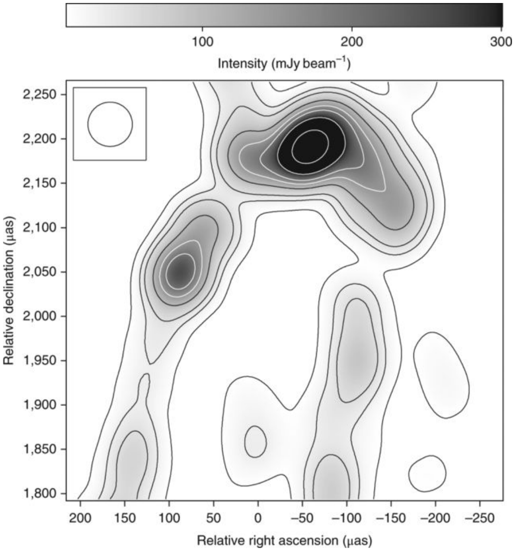

Example: Optical astronomy

Center for High Angular Resolution Astronomy

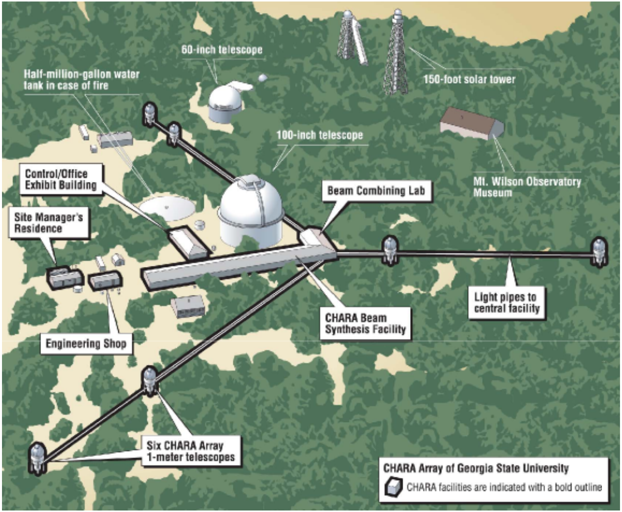

http://www.chara.gsu.edu

Example: Optical interferometry, Algol and Beta Lyrae

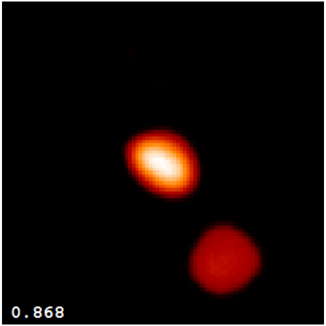

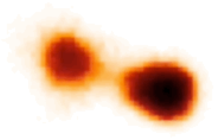

Interacting Binary Beta Lyrae


WRINKLES IN SPACETIME
THE WARPED ASTROPHYSICS OF INTERSTELLAR
BY ADAM ROGERS

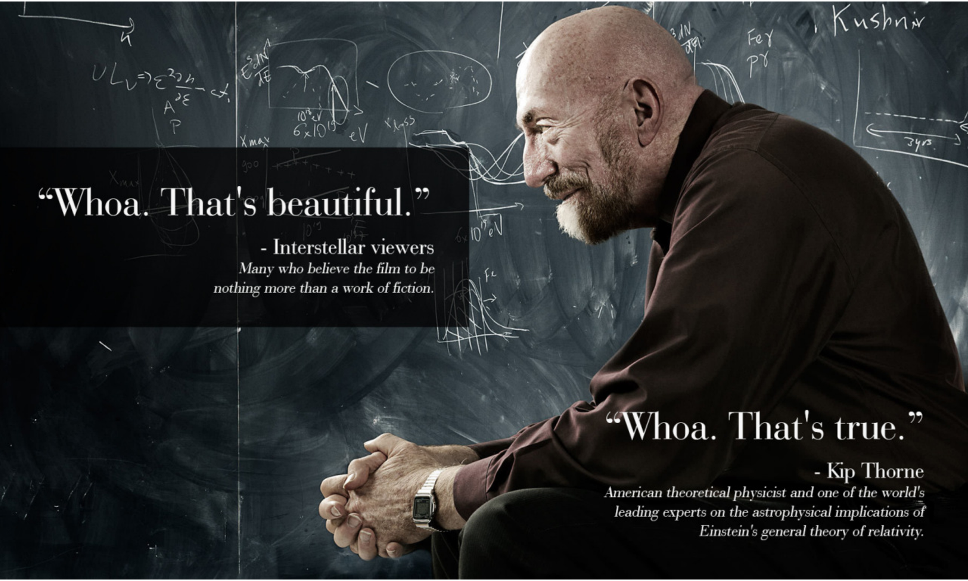
"Whoa. That's beautiful."
- Interstellar viewers
Many who believe the film to be nothing more than a work of fiction.
"Whoa. That's true."
- Kip Thorne
American theoretical physicist and one of the world's leading experts on the astrophysical implications of Einstein's general theory of relativity.

Example: EHT imaging simulation of a black hole in the center of M87, deconvolution

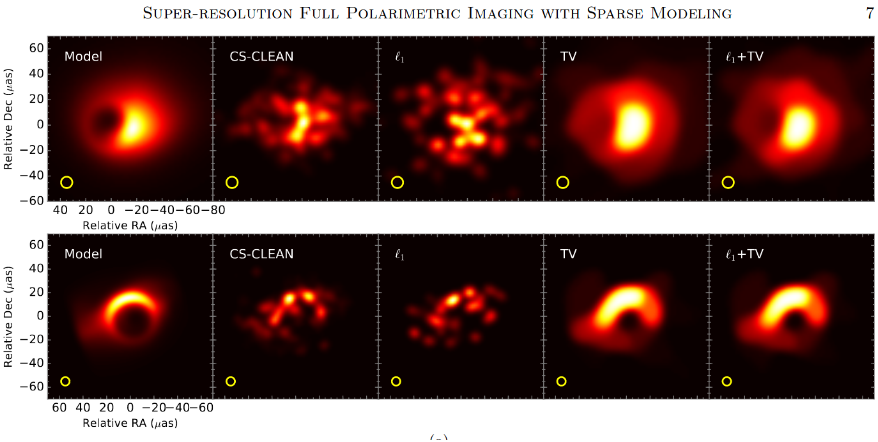

From Akiyama et al. (A&A 2017)

`https://arxiv.org/pdf/1702.00424.pdf`

Example: EHT imaging simulation of a black hole in the center of M87, uv-coverage

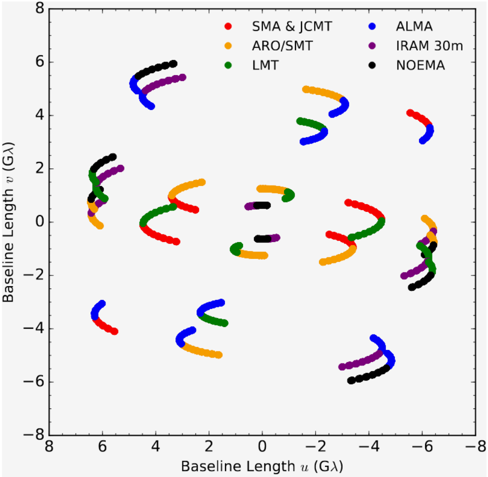

Figure 2. The uv-coverage of the simulated observations. Each baseline is split into two colors to indicate the corresponding two stations.

Simulation software

`https://launchpad.net/apsynsim`